

# An intriguing connection between the Bardeen-Moshe-Bander phenomenon and $2 + p$ spin glasses

Vincent Lahoche<sup>1,\*</sup> and Dine Ousmane Samary<sup>1,2,†</sup>

<sup>1</sup>Université Paris Saclay, CEA, LIST, Gif-sur-Yvette, F-91191, France

<sup>2</sup>Faculté des Sciences et Techniques (ICMPA-UNESCO Chair)  
Université d'Abomey-Calavi, 072 BP 50, Bénin

This paper aims to establish a close connection between the Bardeen-Moshe-Bander phenomenon and a  $p=2+3$  spin-glass model with sextic confinement potential. This is made possible by the unconventional power-counting induced by the effective kinetics provided by the disorder coupling in the large  $N$ -limit. Because of the absence of epsilon expansion, our approach is more attractive than the previous one and may probably play a relevant role in the signal detection issue in nearly continuous spectra.

PACS numbers: 05.10.Cc, 05.10.Gg, 05.70.Fh

*a. Introduction.* The Bardeen-Moshe-Bande (BMB) phenomenon, first discovered thirty years ago, is a surprising and important phenomenon in statistical field theory, particularly in the study of critical phenomena. In this phenomenon, the  $\beta$ -functions of the  $\epsilon$ -expansion of sextic  $O(N)$  models near  $3D$  have a non-trivial large  $N$  limit. In this limit, for  $D = 3$ , there exists an attractive line of fixed points (FP) for the critical theory, starting from the Gaussian fixed point and ending at some special marginal (asymptotically safe) FP [1, 3]. To be more precise the BMB phenomenon can be described shortly by the following: Consider a critical sextic  $O(N)$  model, with classical action in dimension  $D = 3 - \epsilon$ :

$$S_{\text{cl}}[\vec{\phi}] = \frac{1}{2} \int d^D \mathbf{x} \vec{\phi}(\mathbf{x}) \cdot (-\Delta) \vec{\phi}(\mathbf{x}) + \frac{g}{3N^2} \int d^D \mathbf{x} (\vec{\phi}^2(\mathbf{x}))^3, \quad (1)$$

where  $\mathbf{x} \in \mathbb{R}^D$ ,  $\vec{\phi} := \{\phi_1, \dots, \phi_N\}$ , and  $\Delta$  is the standard Laplacian over  $\mathbb{R}^D$ . The perturbative expansion as usual is self-organized in a loop expansion, but due to the special scaling of the sextic interaction, the loop expansion stops at four loops. Indeed, a general Feynman amplitude  $A(G)$  for some 1PI diagram  $G$  scales as  $A(G) \sim N^{-2V+F}$ , where  $V$  is the number of vertices involved in the corresponding diagram, and  $F$  is the number of faces i.e the closed cycles of fields indices, sharing a factor  $N$  (see Fig. 1). Furthermore, imposing the dimensional regularization [2], the tadpoles diagrams must vanish  $\int d^D \mathbf{p} (\mathbf{p}^2)^\alpha = 0$ . Then, considering only the 1PI diagrams, a moment of reflection shows that the number of faces in leading order (LO) graphs depends on the fact that  $V$  is

$$F_{LO} = \begin{cases} \frac{3V}{2} - 2 & \text{if } V = 2n \\ \frac{3(V-1)}{2} & \text{if } V = 2n + 1 \end{cases}. \quad (2)$$

Then, we find that  $A(G) \sim N^{-3}$  for  $V = 2, 3$ , and as  $A(G) \sim \mathcal{O}(N^{-4})$  with  $V > 3$ . The computation of the  $\beta$ -function leads to, taking into account similar quantum corrections for anomalous dimension:

$$N\beta(g) = -2N\epsilon g + 12g^2 - \frac{\pi^2}{2}g^3 + \mathcal{O}(1/N), \quad (3)$$

which has two fixed-point solutions:  $g_{\pm} = 2(6 \pm \sqrt{36 - \pi^2 N \epsilon}) / \pi^2$ . By fixing the value of  $\epsilon$ , the fixed point does not make sense in the large  $N$  limit, except if we assume that  $N\epsilon = \mathcal{O}(1)$  i.e  $\epsilon := \alpha/N$ , and the critical line seems to exist only for dimension  $D \in [D_c(N), 3]$ , where  $D_c(N) := 3 - \pi^2/36N$ . Since the last decade, the BMB phenomenon has been explored and generalized for different fields theories involving for instance fermions and supersymmetry [5, 6]. Furthermore, a finite  $N$  origin has recently been investigated using nonperturbative renormalization [4]. Note that the BMB phenomenon isn't all that new, and is widely used in the literature. However, the connection we point out in this paper with  $2 + p$  spin glass is a novelty that requires special attention. Furthermore, to our knowledge, the first example in which the phenomenon occurs naturally in constructing the large  $N$  limit, without requiring physically disputable methods like dimensional regularization is [7].

*b. The model.* The first model we consider in this letter is a soft  $p = 2$ -spin model, corresponding to the equilibrium probability distribution of the stochastic process:

$$\frac{dq_i}{dt} = - \sum_j W_{ij} q_j - \partial_i V(\vec{q}) + \eta_i(t), \quad (4)$$

where  $\vec{q} \in \mathbb{R}^N$ ,  $\vec{q}^2$  is the Euclidean square length,  $W_{ij}$  are the entries of a  $N \times N$  Wigner symmetric matrix of variance  $\sigma^2$ , and  $\eta_i(t)$  is a Gaussian white noise  $\langle \eta_i(t) \eta_j(t') \rangle = 2T \delta_{ij} \delta(t - t')$ . The potential  $V(\vec{q})$  is defined without arbitrary large spin configurations [8], and includes a disorder contribution:

$$V(\vec{q}) = \sum_{n=1}^{PM} \frac{a_n (\vec{q}^2)^n}{(2n)! N^{n-1}} + \sum_{i_1 < \dots < i_p} J_{i_1 \dots i_p} q_{i_1} \dots q_{i_p}, \quad (5)$$

\*vincent.lahoche@cea.fr

†dine.ousmanesamary@cea.fr

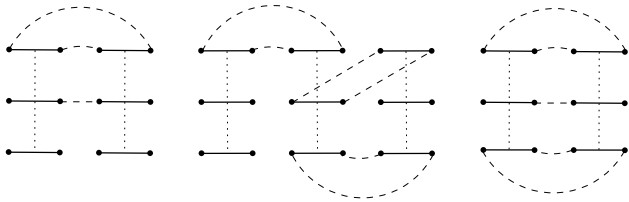


FIG. 1: Typically relevant two and four loops diagrams for the critical sextic theory, for effective coupling (on left) and anomalous dimension (on right). Solid edges materialize scalar products  $\vec{\phi} \cdot \vec{\phi}$ , and vertices are sets of 3 solid edges linked with a dotted edge. Propagators are the dashed edges. A face is an alternate closed sequence of dashed and solid edges.

where  $J_{i_1 \dots i_p}$  is a random tensor with centered independent entries and correlation function:

$$\overline{J_{i_1 \dots i_p} J_{i'_1 \dots i'_p}} = \left( \frac{2\kappa p!}{(2p)! N^{p-1}} \right) \prod_{\ell=1}^p \delta_{i_\ell i'_\ell}, \quad (6)$$

where  $\kappa$  is an arbitrary parameter. This model can be studied analytically in the large  $N$  limit. For  $\kappa = 0$ , it corresponds to the standard  $p = 2$  soft spin model. In this case, despite that the equilibrium dynamics solution does not exhibit a true spin glass phase and is nothing but a ferromagnet in disguise, the out-of-equilibrium problem is not so trivial and exhibits aging effects, for instance, [8–10]. For  $\lambda \neq 0$ , the spherically constrained model can be solved as well using the replica technique [11] at equilibrium. The equilibrium distribution  $P_{\text{eq}}(\vec{q})$  for given samples of  $J$  and  $W$  is  $P_{\text{eq}}(\vec{q}) \propto \exp -H(\vec{q})/T$ , with  $H(\vec{q}) := \frac{1}{2} \sum_{i,j} q_i W_{ij} q_j + V(\vec{q}^2)$ . In the rest of this paper, we set  $T = 1$ . First, let us focus on the case  $\kappa = 0$ . For  $N$  large enough, the spectrum for  $W$  becomes deterministic, and goes toward the Wigner distribution  $\mu_W(\lambda) = \sqrt{4\sigma^2 - \lambda^2}/2\pi\sigma^2$ . We furthermore introduce the positive “generalized momenta” [12]:  $p := \lambda + 2\sigma$ , so that up the mass translation  $\mu_1 := a_1 - 2\sigma$ , the Hamiltonian  $H(\vec{q}) \asymp H_\infty(\vec{\phi})$ , with:

$$H_\infty(\vec{\phi}) := \frac{1}{2} \sum_p^{pM} \phi(p)(p+\mu_1)\phi(p) + \sum_{n=2} \frac{a_n(\vec{\phi}^2)^n}{(2n)! N^{n-1}}. \quad (7)$$

where  $\phi(p) \asymp \sum_i q_i u_i^{(\lambda)}|_{\lambda=p-2\sigma}$ , for some normalized eigenvector  $u_i^{(\lambda)}$  of  $W$ , and  $\vec{\phi}^2 := N \int dp \rho(p) \phi^2(p)$ , where  $\rho(\lambda + 2\sigma) \equiv \mu_W(\lambda)$ . Then, in the large  $N$  limit, the equilibrium distribution looks like an ordinary field theory, with nearly continuous momenta  $p$  and partition function:

$$Z_\infty[j] := \int [d\phi] e^{-H_\infty(\vec{\phi}) + \sum_p \phi(p)j(p)}. \quad (8)$$

*c. Scaling and RG.* Following [12, 14, 16], an unconventional Wilsonian RG [15] can be constructed by

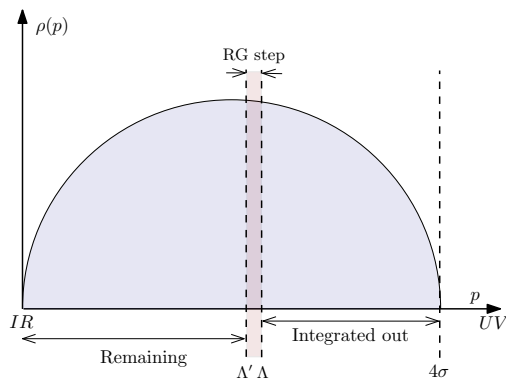


FIG. 2: A typical RG step on the Wigner spectrum.

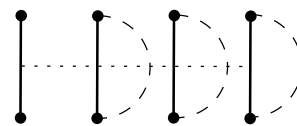


FIG. 3: LO contribution of order  $a_4$  to the self energy.

partially integrating out degrees of freedom in the partition function (8), from UV scales (large  $p$ ) to IR scales (small  $p$ ) – see Fig. 2. Note that there are three differences with ordinary RG: 1) The spectrum is not a power law than in ordinary QFTs. 2) The spectrum is bounded. 3) The sums in the Hamiltonian  $H_\infty$  are without dimension. Accordingly with [12, 17], a canonical notion of dimension can be however defined for coupling regarding the behavior of the RG flow. Indeed, fixing some cut-off  $\Lambda$  on the spectrum,  $\mu_1$  scales as  $p$  with respect to  $\Lambda$  under distribution dilatation.

Now, let us consider the quantum correction to the self-energy of order  $a_n$  (Fig. 3). The corresponding Feynman amplitude scale as  $A(G) \sim (L_1(\Lambda))^{n-1}$ , where  $L_1(\Lambda) \sim \int_0^\Lambda \rho(p)/\Lambda$ , and we define the *canonical scaling*  $I_n(\Lambda)$  of the coupling  $a_n$  such that:

$$I_n(\Lambda)(L_1(0, \Lambda))^{n-1} \sim \Lambda, \quad (9)$$

and the *canonical dimension* as:

$$d_n := \Lambda \frac{d}{d\Lambda} \ln (\Lambda(L_1(0, \Lambda))^{1-n}). \quad (10)$$

For the Wigner law, we get explicitly for the canonical dimension  $d_n^{(0)} = (3 - n)/2$  for  $\Lambda$  small enough ( $\forall \sigma$ ). This power counting matches with the standard power counting of a 3D field theory, because for  $p$  small enough,  $\rho(p) \sim \sqrt{p}$ . In addition with  $\Lambda$  corrections arising because of the shape of the Wigner laws, there are also corrections occurring by the  $1/N$  expansion of the Wigner law [18], and  $d_n$  looks like a series by fixing  $\Lambda$ :

$$d_n = d_n^{(0)} + \frac{1}{N} d_n^{(1)} + \mathcal{O}(1/N^2). \quad (11)$$

We get in the deep IR, for  $\sigma = 0.5^1$ ,  $d_n^{(1)} = \frac{791\Lambda(n-1)}{3645} + \mathcal{O}(\Lambda^{3/2})$  and  $d_n^{(0)} = \frac{3-n}{2} + \frac{3}{20}(n-1)\Lambda + \mathcal{O}(\Lambda^{3/2})$ .

*d. Perturbative  $\beta$ -functions.* In (7) we set  $p_M = 3$  and we compute the LO  $\beta$ -function accordingly with the standard BMB argument. Indeed, the power counting shows that quadratic and quartic couplings are relevant, and counter-terms could be defined in perturbation theory to fine-tune these couplings to zero, following the computation done in [19], and the relevant Feynman diagrams for 1PI 6 and 2-points functions for sextic couplings and anomalous dimension are again given by Fig. 1. To simplify the computation, we decide to use the standard Wetterich formalism [16, 20] by adding a regulator  $\Delta_\Lambda := \frac{1}{2} \sum_p \phi(p) R_\Lambda(p) \phi(p)$  in the effective action, and in the deep IR  $R_\Lambda(p)$  is equivalent to the Litim type regulator<sup>2</sup>  $R_\Lambda(p) \sim (\Lambda - p)\theta(\Lambda - p)$ , where  $\theta$  is the standard Heaviside function [21]. All the diagrams involves powers of the 1-face integral ( $\mu_1 \ll 1$ ):

$$I_2(\mu_1, \Lambda) := \int_0^2 dp \frac{\rho(p)}{(p + \mu_1 + R_\Lambda(p))^2}. \quad (12)$$

The typical spacing between eigenvalues being of order  $1/N$  i.e. of the same order as the effects we are aiming to compute. We can therefore use Wigner distribution in our computation, and we get (assuming again  $\Lambda \ll 1$ ):

$$I_2(\mu_1, \Lambda) = \frac{16\sqrt{2}}{3\pi\sqrt{\Lambda}} + \mathcal{O}(\Lambda^0, \sqrt{\mu_1}). \quad (13)$$

In the rest, we use the standard mass scheme to compute RG equations. Because of the critical condition, the zero momenta 6-points effective vertex function can be computed as:

$$N^3 \Gamma_\Lambda^{(6)} = Na_3 - A(\Lambda)a_3^2 + B(\Lambda)a_3^3 + \mathcal{O}(N^{-1}), \quad (14)$$

and furthermore, the wave function renormalization  $Z$  is defined from the self energy  $\Sigma(p)$  as the first derivative with respect to the external momenta  $p$ , for  $p = 0$ :  $Z := 1 - \Sigma'(0) = 1 - C(\Lambda)a_3^2 N^{-2} + \mathcal{O}(N^{-3})$ . From perturbation theory we get:  $A = I_2/(10\Lambda)$ ,  $B = I_2^3/900$  and  $C = 0$ . Note that the vanishing of  $C$  is a consequence of the choice of the regulator. Then, equation (14) defines the effective coupling  $u_3 = a_3 - (Aa_3^2 - Ba_3^3)N^{-1} + \mathcal{O}(N^{-2})$ . We then define the dimensionless coupling  $u_3 =: \bar{u}_3 I_3(\Lambda)$ ,

and the  $\beta$  function follows [2]:  $\beta := \Lambda \frac{d\bar{u}_3}{d\Lambda}$ . To compute the RHS of this relation, we have to keep in mind that we focus on the deep IR regime  $\Lambda \ll 1$ , and because the spacing between eigenvalues is of order  $1/N$  [24],  $\Lambda = cN^{-1}$ . In particular,  $I_3(\Lambda) = \pi^2/32 + \mathcal{O}(\Lambda)$ , computed with the Wigner law. We get:

$$\beta = - \left( \frac{3}{10} + \frac{1}{N} \frac{1582}{3645} \right) \Lambda \bar{u}_3 + \frac{\sqrt{2}\pi}{40} \bar{u}_3^2 \left[ 1 - \frac{8\bar{u}_3}{405} \right] \frac{\Lambda^{-3/2}}{N} + \mathcal{O}((\Lambda N)^{-2}). \quad (15)$$

Because the typical spacing between eigenvalues is  $\delta \sim N^{-1}$ , we set  $\Lambda = cN^{-\alpha}$  in the deep IR, assuming  $c = \mathcal{O}(1)$ . This allows us to characterize three different regimes. Using (2), we get that Feynman amplitudes scales as  $A(G) \sim N^{\omega(G)}$  with:

$$\omega(G) = \frac{(3\alpha - 2)V(G) - 4\alpha + (1 + \alpha)\theta_{V=2n+1}}{4}, \quad (16)$$

where  $\theta_A = 1$  if  $A$  is true and 0 otherwise. Hence, as  $\alpha \leq 2/3$ , the contributions of higher order diagrams decrease in the large  $N$  limit. Another interesting point is for  $\alpha = 2/5$ , for which the dimensional and LO loop contributions have the same size (i.e.  $\alpha = -3\alpha/2 + 1$ ). For  $\alpha \leq 2/3$ , we find a *marginal fixed line*<sup>3</sup>:

$$\bar{u}_3^{(\pm)} = \frac{405}{16} \left( 1 \pm \sqrt{1 - \frac{64\sqrt{2}c^{5/2}}{135\pi} N^{1-5\alpha/2}} \right). \quad (17)$$

For  $\alpha \geq 2/5 = 0.4$ , the fixed point line is arbitrary close to  $\bar{u}_3^* := 40.5$  as  $c = \mathcal{O}(1)$ , and  $c \ll (\pi\sqrt{2}/192)^{\frac{2}{5}} N^{\alpha - \frac{2}{5}}$ . Finally for  $\alpha < \alpha_c(N)$ , the fixed point solution break down, with:

$$\alpha_c(N) := \frac{2}{5} - \frac{K}{\ln N}, \quad K := \ln \left( \frac{135\pi}{64\sqrt{2}} c^{5/2} \right). \quad (18)$$

Above this value, the dimensional contribution  $-3\Lambda\bar{u}_3/10$  dominates the flow and  $\bar{u}_3 \sim \exp(-\frac{3}{10}\Lambda)$  (exponential regime). Fig. 4 summarizes the different regions. Note that, as  $\alpha > 2/3$  (nonperturbative regime) higher order contribution cannot be discarded, and nonperturbative techniques are required to prove whether the fixed line exists or not.

---

*e. 2+3 spin glasses.* Let  $\overline{Z_\infty^n}$  be the averaging of the replicated partition function [10, 22]:

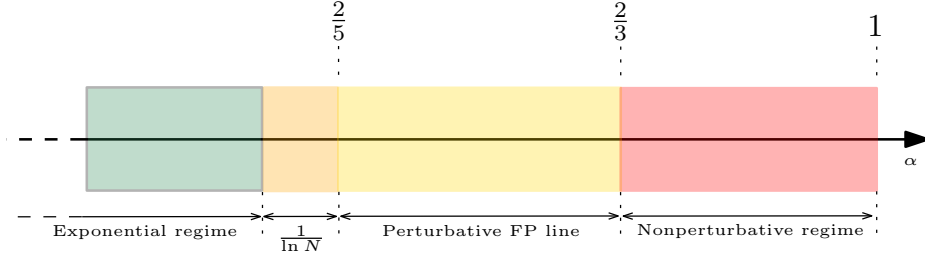


FIG. 4: Summary of the different IR regimes

$$\overline{Z}_\infty^n = \int \prod_\alpha [d\phi_\alpha] \exp \left( - \sum_{\alpha=1}^n H_\infty(\vec{\phi}_\alpha) - W_\infty + \sum_{p,\alpha} \phi_\alpha(p) j_\alpha(p) \right), \quad (20a)$$

where Greek letters are for replica indices, and

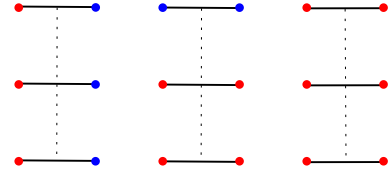
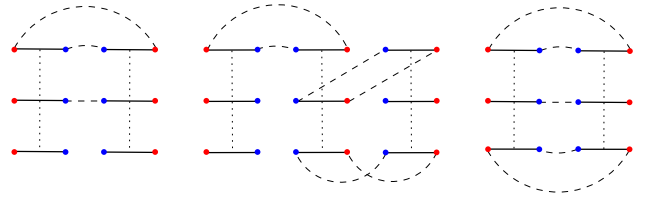
$$W_\infty := - \frac{\kappa}{(2p)! N^{p-1}} \sum_{\alpha,\beta} \sum_p (\phi_\alpha(p) \phi_\beta(p))^p. \quad (21)$$

We consider the case  $p = 3$ , again in the critical regime, where quartic and quadratic local counter-terms are adjusted to cancel the corresponding asymptotically relevant observables. Note that the replica symmetry is explicitly broken in the expression above because of the source terms [10, 23]. To deal with multi-replica vertices, we change our notation and adopt the convention that nodes marked with the same color on a vertex or on a graph have the same replica indices. Fig. 5 shows the three interactions we can construct at the leading order, with three faces (all of them scales as  $N^{-2}$ ). Fig. 6 shows typical contributions for the couplings  $\lambda$  and  $\lambda'$ , involving multi-replica vertices. The  $\beta$ -functions can be computed from the same method as before, and with some efforts, we get  $Z = 1$  again and (again, bares are for dimensionless couplings):

$$\begin{aligned} \beta_{u_3} = & \beta + \frac{\sqrt{2}\pi}{40} \frac{\Lambda^{-3/2}}{N} \left( \frac{\bar{\lambda}^2}{2} - 2\bar{\lambda}\bar{u}_3 \right) \\ & - \frac{\sqrt{2}\pi}{2025} \frac{\Lambda^{-3/2}}{N} \left( \frac{\bar{\lambda}^3}{4} + 3\bar{\lambda}^2\bar{u}_3 - 3\bar{\lambda}\bar{u}_3^2 \right) + \mathcal{O}((\Lambda N)^{-2}), \end{aligned} \quad (22)$$

$$\beta_\lambda = -\frac{3}{10} \Lambda \bar{\lambda} + \frac{\sqrt{2}\pi}{2025} \frac{\Lambda^{-3/2}}{N} \frac{\bar{\lambda}^3}{16} + \mathcal{O}((\Lambda N)^{-2}), \quad (23)$$

$$\beta_{\lambda'} = -\frac{3}{10} \Lambda \bar{\lambda}' + \frac{\sqrt{2}\pi}{80} \frac{\Lambda^{-3/2}}{N} \bar{\lambda}^2 + \mathcal{O}((\Lambda N)^{-2}). \quad (24)$$

FIG. 5: The three relevant effective sextic interactions, that we denote respectively as  $\lambda$ ,  $\lambda'$ , and  $u_3$  (as previously).FIG. 6: Relevant contributions for  $\beta_\lambda$  and  $\beta_{\lambda'}$  (respectively on the middle and the left) and for  $\Sigma$  (on right). Nodes marked with the same color have the same replica index.

The equation (23) can be easily solved, and in the windows of momenta  $\alpha \in [\alpha(N), 2/3]$ ,  $\bar{\lambda}$  is almost constant for  $N$  large enough  $\bar{\lambda} \approx \bar{\lambda}(0)/0.55$ , the initial condition being assumed in the IR regime, so that the equation (23) makes sense. Note that we have to keep in mind that the initial condition for  $\bar{\lambda}$  assumes  $\bar{\lambda}(0) < 0$ , but we will look at the state of the phase space in its entirety, including also the positive region. This region no longer has an interpretation in terms of a theory with disorder of type  $2 + p$ , but could be accessible by nonperturbative methods beyond the scope of this article. We will therefore study it in anticipation of subsequent results.

Analyzing the zeros of  $\beta_{u_3}$ , we get three fixed lines in the large  $N$  limit (but focusing on the interval  $\alpha \in$

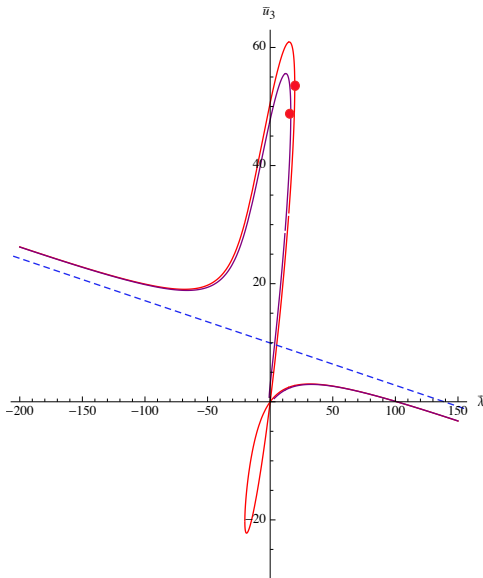


FIG. 7: Fixed lines in the space  $(\bar{u}_3, \bar{\lambda})$ , in the large  $N$  limit, for  $\alpha = 1/2$  (red curve) and  $\alpha = 2/5$  (purple curve).

$[\alpha(N), 2/3]$ , depending on the value of  $\bar{\lambda}$  as Fig. 7 shows. In Fig. 9 we show the corresponding critical exponents and their dependency on  $\bar{\lambda}$ . The red line corresponds to the critical exponents along the unbounded fixed-line. It is in the positive region, and the line is repulsive. The two last curves correspond to the critical exponents along the two pieces of the bounded fixed lines. The upper part (until the red dot on Fig. 7) corresponding to the purple curve in Fig. 9 has a positive exponent and is global *repulsive*, and the second part below the dot (blue curve) has a negative exponent and behaves as a worldwide *attractor*. The repulsive line introduces a discontinuity in the phase space, reminiscent of a first-order phase transition, and the discontinuity point marked by the red dot identifies with a critical point.

*f. Conclusion.* To summarize this letter, we showed that the effective kinetics occurring in the large  $N$  limit for  $p$ -spin glasses involving a matrix-like disorder allows an intriguing connection with the BMB phenomenon for sextic theories. For  $p = 2$ , with a sextic confining potential, we show the existence of a fixed line in the IR, in the domain  $\alpha \in [\alpha_c(N), 2/3]$ . The same kind of phenomenon occurs for the 2 + 3 spin model, and the transition be-

Finally, analyzing the global zeros of the  $\beta$  functions, we get a global fixed line, for:

$$\bar{\lambda} = -18\sqrt{\sqrt{2}\frac{15}{\pi}}N^{\frac{1}{2}(1-\frac{5\alpha}{2})}. \quad (25)$$

Each point of this line is a Wilson-Fisher-like fixed point, with one relevant direction and one irrelevant direction (see Fig. 8). For  $N$  large enough and  $\alpha = 2/3$ , the critical exponent along the relevant direction is found numerically almost independent of  $N$ ; we have for instance  $\theta_{\text{WF}} \approx 5.18$  for  $N = 10^5$  and the large  $N$  limit value is numerically estimated as  $\theta_{\text{WF}}^{\infty} \approx 5.62$ . For the irrelevant direction, the critical exponent behaves as  $-3N^{-\alpha}/5$ , and goes to zero for  $N$  large enough, meaning that the direction tends to begin marginal. The critical line, in that case, separates between a regime with vanishing  $\bar{\lambda}$  (ordered phase) and a regime with non-vanishing  $\bar{\lambda}$  (disordered phase), where replica symmetry breaking is en-

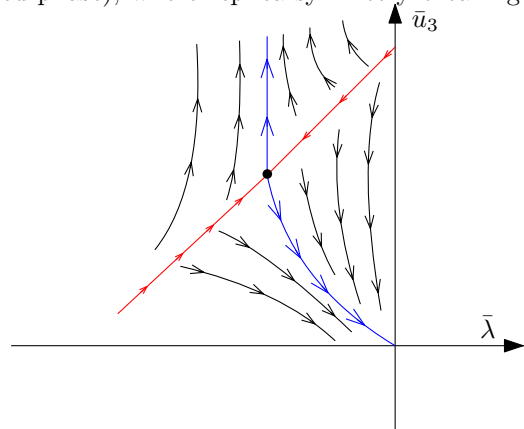


FIG. 8: Qualitative picture of the phase space around the Wilson-Fisher in the negative region for  $\bar{\lambda}$ .

forced.

tween the symmetric or broken replica phase is recovered. Nonperturbative techniques seem however to be required to investigate the deep IR regime  $\alpha \in (2/3, 1)$ , which will be the topic of a forthcoming work. The same kind of phenomena is expected for the effective field theories we recently considered for signal detection issues in nearly continuous spectra [12, 13], and we plan to investigate this point for future work.

[1] William. A. Bardeen, Moshe. Moshe and Myron. Bander Physical Review Letters, 52(14), 1188.  
[2] Jean. Zinn-Justin. (2007). Oxford University Press, USA.

[3] Hugh. OSBORN and Andreas. STERGIOU. arXiv preprint arXiv:1707.06165, 2017.  
[4] Claude. Fleming, Bertrand. Delamotte, and Shun-

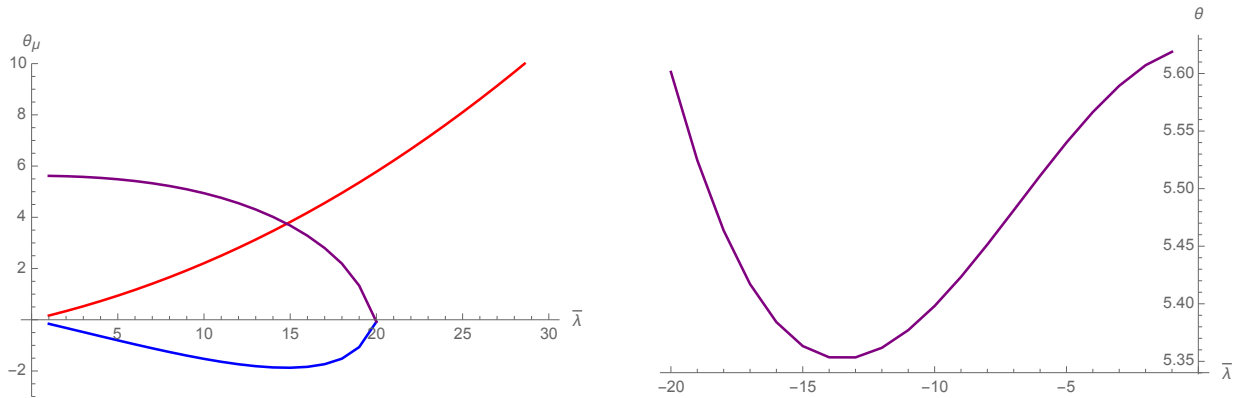


FIG. 9: Dependency of the critical exponents  $\theta_\mu$  ( $\mu = 1, 2, 3$ ) with respect to  $\bar{\lambda}$  along the two pieces of the bounded fixed line (blue and purple curves) and along the unbounded line (red curve). ( $\alpha = 2/3$ ).

- suke. Yabunaka. *Physical Review D* 102.6 (2020): 065008.
- [5] Tsuneo. Suzuki. *Phys. Rev. D* 32, 1017 (1985)
- [6] Tsuneo. Suzuki and Hisashi. Yamamoto. *Prog. Theor. Phys.* 75, 126 (1986).
- [7] Jonathan F. Schonfeld. *The European Physical Journal C* 76.12 (2016): 710.
- [8] Vincent. Lahoche and Dine. Ousmane Samary. *The European Physical Journal Plus* 138.5 (2023): 1-10.
- [9] Leticia F. Cugliandolo and David S. Dean. *Journal of Physics A: Mathematical and General* 28.15 (1995): 4213.
- [10] Cirano. De Dominicis and Irene. Giardina. Cambridge University Press, 2006.
- [11] Andrea. Crisanti and Luca. Leuzzi. *Physical review letters* 93.21 (2004): 217203.
- [12] Vincent. Lahoche, Dine. Ousmane Samary and Mohamed. Tamaazousti. *Journal of Statistical Mechanics: Theory and Experiment* 2022.3 (2022): 033101.
- [13] Vincent. Lahoche, Dine. Ousmane Samary and Mohamed. Tamaazousti. *arXiv preprint arXiv:2201.04250* (2022).
- [14] Serena. Bradde and William. Bialek. *Journal of statistical physics* 167 (2017): 462-475.
- [15] Kenneth G. Wilson. *Reviews of Modern Physics* 55.3 (1983): 583.
- [16] Vincent. Lahoche and Dine. Ousmane Samary. *arXiv preprint arXiv:2403.07577*.
- [17] Vincent. Lahoche and Dine. Ousmane Samary. *Physical Review D* 98.12 (2018): 126010.
- [18] Gurjeet S. Dhesi, and Jones R. Clark. *Journal of Physics A: Mathematical and General* 23.23 (1990): 5577.
- [19] Robert D. Pisarski. *Physical Review Letters* 48.9 (1982): 574.
- [20] Juergen. Berges, Nikolaos. Tetradis, and Christof. Wetterich. *Physics Reports* 363.4-6 (2002): 223-386.
- [21] Daniel F. Litim. *Physical Review D* 64.10 (2001): 105007.
- [22] Marc. Mézard, Giorgio. Parisi and Miguel. Angel. Virasoro. Vol. 9. World Scientific Publishing Company, 1987.
- [23] G. Tarjus and M. Tissier. *Physical Review B* 78.2 (2008), p. 024203
- [24] L. Erdos, B. Schlein, H.T. Yau. *Comm. Math. Phys.* 287 (2009) 641